NASA
Technical Memorandum 103098

AVSCOM
Technical Report 90-C-008

# Matrix Density Effects on the Mechanical Properties of SiC/RBSN Composites



Ramakrishna T. Bhatt
*Propulsion Directorate*
*U.S. Army Aviation Research and Technology Activity—AVSCOM*
*Lewis Research Center*
*Cleveland, Ohio*

and

James D. Kiser
*Lewis Research Center*
*Cleveland, Ohio*



Prepared for the
14th Annual Conference on Composites and Advanced Ceramics
sponsored by the American Ceramic Society
Cocoa Beach, Florida, January 15-19, 1990

NASA

US ARMY
AVIATION
SYSTEMS COMMAND
AVIATION R&T ACTIVITY

# MATRIX DENSITY EFFECTS ON THE MECHANICAL PROPERTIES OF SiC FIBER REINFORCED SILICON NITRIDE MATRIX COMPOSITES

Ramakrishna T. Bhatt
Propulsion Directorate
U.S. Army Aviation Research and Technology Activity - AVSCOM
Lewis Research Center
Cleveland, Ohio 44135

and

James D. Kiser
National Aeronautics and Space Administration
Lewis Research Center
Cleveland, Ohio 44135



## SUMMARY

The room temperature mechanical properties were measured for SiC fiber-reinforced reaction-bonded silicon nitride composites (SiC/RBSN) of different densities. The composites consisted of ~30 vol % uniaxially aligned 142 μm diameter SiC fibers (Textron SCS-6) in a reaction-bonded $Si_3N_4$ matrix. The composite density was varied by changing the consolidation pressure during RBSN processing and by hot isostatically pressing the SiC/RBSN composites. Results indicate that as the consolidation pressure was increased from 27 to 138 MPa, the average pore size of the nitrided composites decreased from 0.04 to 0.02 μm and the composite density increased from 2.07 to 2.45 gm/cc. Nonetheless, these improvements resulted in only small increases in the first matrix cracking stress, primary elastic modulus, and ultimate tensile strength values of the composite. In contrast, HIP consolidation of SiC/RBSN resulted in a fully dense material whose first matrix cracking stress and elastic modulus values were ~15 and ~50 percent higher, respectively, and ultimate tensile strength values were ~40 percent lower than those for unHIPed SiC/RBSN composites. The modulus behavior for all specimens can be explained by simple rule-of-mixture theory. Also, the loss in ultimate strength for the HIPed composites appears to be related to a degradation in fiber strength at the HIP temperature. However, the density effect on matrix fracture strength was much less than would be expected based on typical monolithic $Si_3N_4$ behavior, suggesting that composite theory is indeed operating. Possible practical implications of these observations are discussed.

E-5306

## INTRODUCTION

For heat engine applications, fiber-reinforced ceramic matrix composites are being developed that are strong, tough, and stable in an oxidizing environment at temperatures to possibly as high as 1600 °C. This new class of materials offers the promise of maintaining the advantages of monolithic ceramics, namely, low density, high temperature strength, and oxidation resistance, while providing microstructural mechanisms for improved toughness. Several fiber-reinforced ceramic matrix composite systems are being developed (refs. 1 to 3). One system that shows promise for high temperature application is a SiC fiber-reinforced reaction-bonded silicon nitride matrix composite (SiC/RBSN)

(ref. 3). In the as-fabricated condition this composite displays a metal-like stress-strain behavior, graceful failure beyond matrix fracture, and strength properties superior to that of unreinforced RBSN of comparable density. However, the composite shows less than optimum first matrix fracture stress (ref. 4) and, because of the porous nature of the RBSN matrix (~30 percent porosity), displays a loss in mechanical properties after long term exposure in an oxidizing environment in the 600 to 1000 °C range (ref. 3). By increasing the matrix density, it is expected that oxidation resistance and possibly matrix strength can be substantially improved.

This study had three objectives: (1) to improve the composite density of the SiC/RBSN composites by controlling fabrication variables, (2) to study the influence of improved matrix density on the room temperature mechanical properties of the composite, and (3) to determine the practical advantages of a composite with increased matrix density. The oxidative stability of densified SiC/RBSN composites was not determined and will be discussed in a separate study. Improvement in composite density was achieved by two methods: (1) by increasing the green density of the preform which led to improved nitrided density and (2) by HIP consolidation of the nitrided bodies. The composites were then characterized for density, porosity, and room temperature mechanical properties.

## EXPERIMENTAL

### Composite Fabrication

The starting materials for SiC/RBSN composite fabrication were double-coated SCS-6 SiC monofilaments of nominal diameter 142 μm and commercial grade silicon powder of average particle size 10 μm. The silicon carbide fiber was obtained from Textron specialty Materials and the silicon powder, from Union Carbide. The as-received silicon powder was ground in an attrition mill to reduce its average particle size from 10 to 0.3 μm. A detailed description of the composite fabrication has been described previously (ref. 5). Briefly, the composites were fabricated by three steps. In the first step, SiC fiber mats and silicon cloth tapes were prepared. Those silicon tapes used primarily for SiC/RBSN composites contained 2.5 wt % NiO (a nitridation enhancing additive), while those tapes used for HIPed SiC/RBSN composites contained 2.5 wt % NiO + 5 wt % MgO (a sintering additive). In the second step, alternate layers of SiC fiber mats and the silicon cloths were stacked in a metal die and pressed in a vacuum hot press under an applied stress from 27 to 138 MPa for up to 1 hr in the temperature range from 600 to 1000 °C. In the third step, the consolidated SiC/Si preforms were heat treated in a high purity (>99.99 percent) nitrogen environment in the temperature range from 1000 to 1400 °C for up to 100 hr to convert them to SiC/RBSN composites. The typical dimensions of the as-nitrided composite panels were 150 by 50 by 3.0 mm.

The SiC/RBSN composite panels that contained NiO plus MgO additives were further densified by HIP consolidation. For this purpose, composite panels were coated with a BN slurry and wrapped with 0.25-mm thick grafoil, and then placed over a grafoil wrapped silicon carbide plate of dimension similar to that of the composite panel. The silicon carbide back plate prevented warping of the composite panel during HIPing. The panel and SiC plate assembly was placed into a tantalum can whose inside surfaces were also coated with a BN

slurry. The BN slurry prevented reaction between the tantalum can and the grafoil. The cans were electron beam welded, then leak checked by placing the cans under He at a pressure of 0.69 MPa, followed by immersion in alcohol. The observation of bubbles indicated a leaky can.

The sealed cans were placed inside a graphite element HIP furnace and HIPed for 1 hr at 1850 °C under an argon pressure of 138 MPa. The furnace temperature was monitored with W5Re-W26Re thermocouples having high purity BN insulation. The temperature was controlled with an accuracy of ±10 °C. After HIPing, the Ta cans were cut open to remove the specimens.

The physical and mechanical properties for the as-fabricated and HIPed SiC/RBSN composites were measured at room temperature. For pore size and density measurements, the mercury intrusion method was used.

### Specimen Preparation and Testing

For mechanical property measurements, both as-fabricated and HIPed composite panels were surface ground and cut into 125 by 12 by 2 mm tensile specimens using diamond impregnated grinding and cut-off wheels. The tensile specimens were adhesively bonded with glass fiber-reinforced epoxy tabs at their ends, leaving 25 mm as the test gauge length. A wire wound strain gauge was adhesively bonded to the specimen gauge section for monitoring axial strains. The tensile specimens were tested at room temperature in an Instron machine at a crosshead speed of 1.3 mm/min. For each processing condition, three to five specimens were tested. The fractured specimens were examined using optical and scanning electron microscopy to determine composite failure behavior.

Individual SCS-6 fibers, both as-received and those exposed to the HIPing environment, were prepared for room temperature tensile testing by forming aluminum foil clamps at each end of the fiber, leaving 25 mm as the gauge length. The aluminum foils were inserted in the pneumatic grips, and the fiber specimens were pulled to failure using an Instron at a constant crosshead speed of 1.3 mm/min.

### Microstructural Characterization

Polished cross sections of the composites were prepared for microstructural analysis by grinding the specimens successively on 40, 30, 15, 10, 6, and 3 μm diamond impregnated metal discs, followed by polishing them in a vibratory polisher on microcloth using 0.03 μm diamond powder. The polished specimens were ultrasonically cleaned in alcohol, dried, and sputter coated with a thin layer of pyrolytic carbon. These specimens were examined in a scanning electron microscope.

## RESULTS

### SiC/RBSN Composites

Physical properties. - The variations of average pore size and the bulk density with preform consolidation pressure are shown in figures 1 and 2 for

SiC/RBSN composites before and after nitridation. Each data point represents an average value for five measurements. The scatter in the data represents one standard deviation. Figure 1 shows that as the consolidation pressure is increased, the average pore size of the preform decreased continuously. Furthermore, these preforms after nitridation showed further reduction in average pore size. The general trend of the pore size variation with consolidation pressure for the nitrided panels was similar to that of the preforms. With increase in consolidation pressure, the average pore size of the nitrided bodies initially decreased drastically and then reached a plateau. The densities of both the preform and nitrided composites increased with increasing consolidation pressure (fig. 2)

Microstructural analysis. - For microstructural analysis, the nitrided composite specimens were sectioned normal to the fibers, polished, and then examined using an SEM. Typical SEM micrographs of cross sections of the composites consolidated at 28, 69, and 138 MPa are shown in figure 3. The micrograph of the composite, consolidated at 28 MPa, revealed large voids and cracks between fibers, especially in the plane parallel to the fiber array possibly due to poor infiltration of silicon powder between the fibers. The cross section of the composite, consolidated at 69 MPa pressure, showed very few matrix cracks, but nonuniform distribution of porosity was still prevalent. Again, larger pores and lower density regions were found between the fibers. At the highest consolidation pressure the overall microstructure of the composite appeared similar to the previous case, except for some isolated pockets of unreacted silicon normal to the fiber array. It is also noticeable from these micrographs that as the consolidation pressure is increased, the average pore size decreased and the integrity of the carbon-rich surface coating on SCS-6 SiC fibers remained intact.

Mechanical properties. - A representative room temperature stress-strain curve for a unidirectionally reinforced SiC/RBSN composite fabricated at 69 MPa is shown in figure 4. Similar stress-strain curves were seen for composites consolidated at other pressures. Figure 4 shows three regions: two linearly elastic regions and a nonlinear region. The slope of the initial linear region and the stress at the first point of the deviation are referred to as the primary elastic modulus and the first matrix cracking stress of the composite, respectively. From the stress-strain curves of the composites consolidated at the three different pressures, the primary elastic modulus, the first matrix cracking stress, and the ultimate composite tensile strength were determined. These results, plotted in figure 5, indicate no significant changes in the values of these three key properties with increasing consolidation pressure.

## HIPed SiC/RBSN Composites

Microstructure. - The SEM micrograph of a representative cross section of a HIPed SiC/RBSN composite (fig. 6(a)), shows that HIPed composites display a uniform microstructure with little matrix porosity. The density variations and large voids as seen in the unHIPed composites (fig. 3) are completely eliminated in the HIPed composites. The matrix is uniformly infiltrated between the interstices of the fibers. Higher magnification photographs of the interfacial regions of the unHIPed and HIPed SiC/RBSN composites (figs. 6(b) and (c), respectively) indicate that the carbon-rich coating on the SCS-6 fiber is

physically intact after HIP consolidation. No chemical reaction between the fiber coating and the $Si_3N_4$ matrix was detected.

Mechanical properties. - The room temperature tensile stress-strain curve for the unidirectionally reinforced HIPed SiC/RBSN is shown in figure 7. For comparison purposes, included in the figure is the stress-strain curve for the unHIPed SiC/RBSN composite containing HIPing additive. The shape and general features of the two stress-strain curves are similar. In both cases, the nonlinearity in the stress-strain curves was observed to start with the onset of matrix cracks normal to the fibers. Comparison of the stress-strain curves in the figure indicates that HIPed composites had a higher primary elastic modulus and first matrix cracking stress than the unHIPed composites, but the ultimate tensile strength and strain for the HIPed composites were significantly lower. A summary of the physical and mechanical properties for the HIPed and unHIPed SiC/RBSN is presented in table I.

Tensile specimens that were pulled to failure were examined using an optical microscope. A representative fractured tensile specimen of HIPed SiC/RBSN is shown in figure 8 along with that of the unHIPed SiC/RBSN composite. It is obvious from figure 8 that the fractured HIPed composites showed limited fiber pull-out. The denser matrix helped in retaining the fracture features of the specimen. In contrast, fractured unHIPed composites displayed broomy fracture with limited matrix around the fibers.

In general, the ultimate tensile strength of a unidirectional composite depends on the intrinsic bundle strength of the fibers with a bundle gauge length dependent on the fiber-matrix interfacial shear strength. Therefore any major loss in ultimate tensile strength can be primarily attributed to loss in fiber strength. Removal of fibers from the composite is difficult because the solvents used to dissolve the matrix (for example, a mixture of HF and $HNO_3$) also attack the fibers. This creates a flaw distribution that is different from that of the fibers in the composite. To determine if fiber strength degradation can occur during HIPing, a batch of 20 individual SCS-6 silicon carbide fibers were heat treated at 1850 °C for 1 hr in the HIP furnace and then tensile tested at room temperature. Apart from the heat-treated fibers, a batch containing 20 as-received SiC fibers were also tensile tested to generate baseline strength data. The average tensile strengths of individual fibers before and after heat treatment were 3.79 and 0.82 GPa, respectively. Although the strength of fibers exposed to the HIP conditions may not reflect the true strength of the fibers in the composite, these data show a strength trend which strongly suggests that loss in ultimate tensile strength of the HIPed composite was probably caused by thermally-induced fiber strength degradation.

The effect of matrix density on the interfacial shear strength was also determined. The interfacial shear strength between the fiber and the matrix was determined from the modified Aveston, Cooper, and Kelly (ACK) theory (ref. 6) using experimentally determined average matrix crack spacing values. For measuring average matrix crack spacing, composite specimens were loaded above the nonlinear region, unloaded, and then observed using an optical microscope. The average matrix crack spacing for as-fabricated SiC/RBSN and HIPed SiC/RBSN composites were 0.8±0.2 and 1.0±0.4 mm, respectively. Using appropriate elastic constants for the SiC fibers (ref. 7), RBSN matrix (ref. 4), $Si_3N_4$ matrix (ref. 8), and the matrix crack spacing values for the unHIPed and HIPed SiC/RBSN composites in the ACK equation (ref. 6), the interfacial shear

strength was calculated. The calculated values for SiC/RBSN and HIPed SiC/RBSN were 18±3 and 19±6 MPa, respectively. This suggests that interfacial shear strength between the SiC fiber and the $Si_3N_4$ is not affected by the densification of the matrix.

The overall effect of composite density on the primary elastic modulus and the first matrix cracking stress for the unHIPed and HIPed SiC/RBSN composites is illustrated in figure 9. The dashed line represents the predicted variation of primary elastic modulus with density using simple rule-of-mixtures theory. (The details of this calculation are reported in a later section.) As expected, as the density of the composite is increased, the elastic modulus is also increased. However, in contrast to typical monolithic $Si_3N_4$ behavior, the large density increase for the composite resulted in only small increase in first matrix cracking strength.

## DISCUSSION

Previous RBSN processing studies (refs. 8 to 10) have shown that the density of a monolithic RBSN material depends on the density of the silicon preform. Specifically, the higher the green density of the silicon preform, the higher is the nitrided density. Furthermore, with increasing nitrided density, the elastic modulus of RBSN bodies increased linearly (ref. 10). Although some studies have reported increased room temperature bend strength with increasing RBSN density (refs. 11 and 12), in some cases correlation between strength and density may not be observed because strength, in general, is controlled by the largest critical flaw.

Similar to monolithic RBSN, the density of the SiC/RBSN composites can be improved by increasing preform density. Improved composite density should yield improved primary elastic modulus. This modulus value can be predicted from rule-of-mixtures knowing the elastic moduli and volume fractions of the constituents of the composite. Using $E_f$ = 390 GPa (ref. 7), estimated $E_m$ values of 90 to 120 GPa for RBSN densities ranging from 1.67 to 2.21 gm/cc (ref. 10) (corresponding to SiC/RBSN composite density range from 2.07 to 2.45 gm/cc) and $V_f$ = 0.3, rule-of-mixtures theory predicts elastic modulus values in the range of 180 to 200 GPa for the SiC/RBSN composites. The predicted values, as shown by the dotted line in figure 9, agree well with the measured values.

Such an improvement in composite density, however, had no significant effect on the first matrix cracking strength of the composite. This in part might be explained by ceramic composite fracture theory (ref. 13, appendix) which can predict a weak dependence for cracking stress on matrix density assuming the interfacial shear strength between the fiber and matrix remains the same. Another possible explanation is that the flaw population in the RBSN matrix remained nearly the same. Microstructural results confirm that density variations and voids existed in composites with differing densities. The reason for these microstructural inhomogeneities can be traced to the early stages of fabrication. In the preform stage, the silicon tape containing polymer fugitive binder was forced between the fiber array by uniaxial pressing. The degree to which the silicon tape deforms around the fibers and fills the interfiber cavities depends on the viscoelastic properties of the tape. If uniform packing of silicon powder is not achieved at this stage, it may not be achieved

at a later stage because of the limited plasticity of silicon particles after the polymer fugitive binder is burned out. In addition, the dense fibers restrict the deformation of the silicon. Both of these factors promote nonuniform packing of particles around the fibers, leading to density variations. However, by modifying the fabrication approaches and by controlling the initial particle size distribution of the silicon powder, one should be able to achieve homogeneous microstructure and higher densities. Of course with RBSN processing alone one cannot achieve fully dense material because of the difficulty in complete conversion of silicon to silicon nitride in preforms having densities greater than 85 percent of the theoretical value. For complete conversion of silicon to silicon nitride, continuous and open pore channels are required in RBSN preform bodies. As the green density increases, the total pore content and continuity of pore channels decreases. This promotes unreacted silicon islands in the nitrided bodies. Thus there is a limitation on densification. The presence of large amounts of metallic silicon in the SiC/RBSN composites may also reduce their potential for high temperature use.

In contrast, HIPed SiC/RBSN composites had a fully densified matrix with uniform microstructure, minimum porosity, and negligible free silicon. At the HIPing temperature, the MgO additive reacts with silica and silicon nitride to form a liquid phase (refs. 14 and 15) which allows the matrix to flow uniformly around the fibers and remove any inhomogeneity in microstructure. As shown in figure 9, the HIPed composites showed measurably higher primary elastic modulus and first matrix cracking strength values compared to those for the porous RBSN composites. The higher primary elastic modulus value for the HIPed composites can be explained by the higher matrix modulus due to higher matrix density, and the rule of mixtures. Although the HIPed composites demonstrated improved matrix fracture stress, they showed strain to first matrix cracking stress lower than that for the unHIPed SiC/RBSN (table I). This degradation in strain is in contrast to typical monolithic silicon nitride ceramics in which improved density generally results in increased matrix fracture strain (ref. 10). However, as discussed above, this behavior may be explained by composite theory (refs. 6 and 13, appendix). It can also be concluded that the observed improvement in first matrix cracking stress for the HIPed SiC/RBSN composites can be attributed primarily to increased composite modulus and not due to enhancement of matrix fracture strain as observed; for example, with small diameter (<10 μm) SiC fiber-reinforced glass matrix composites (ref. 16).

Finally, the degradation in ultimate tensile strength of the HIPed composites can be attributed to loss in ultimate tensile strength of SCS-6 fibers during HIP consolidation. Even though the mechanisms of fiber strength degradation are not fully understood, some of the possible underlying mechanisms are annealing of growth related residual stresses, coarsening of SiC grains, chemical changes in the fiber surface coating, and depletion of free silicon in the SiC grain boundaries (ref. 17).

The mechanical property data reported here for HIPed SiC/RBSN agrees well with the data for SiC/$Si_3N_4$ composites fabricated by hot pressing (ref. 18). The implication of this finding is that fully dense SiC/$Si_3N_4$ composites fabricated by two different high temperature fabrication techniques yield similar properties. From a practical point of view, however, subtle differences between these fabrication methods exist; the RBSN/HIP method may allow one to fabricate complex shape components, whereas hot pressing technique is limited to simple shapes.

Finally, the results of this study clearly indicate that with increase in composite density from 2.07 to 3.05 gm/cc, the SiC/RBSN composite showed ~50 percent improvement in the primary elastic modulus and ~15 percent increase in the first matrix cracking stress. However if we normalize the data based on density, we do not observe any appreciable improvement in composite performance. However, one of the expected major advantages of a fully densified composite should be improved oxidative stability.

## SUMMARY OF RESULTS

The room temperature mechanical properties for SiC/RBSN composites that were densified up to the theoretical value have been measured. The major findings are as follows:

(1) The green density of SiC/RBSN preforms can be improved by consolidating them at increasing pressures. The higher green density also yields higher nitrided density. However, improved composite density resulted in only slightly improved primary elastic modulus and first matrix cracking strength.

(2) Fully dense SiC/RBSN composites can be fabricated by HIP consolidation using a sintering additive. The HIPed SiC/RBSN composites showed higher primary elastic modulus and matrix cracking strength than unHIPed SiC/RBSN composites, and, similar to the unHIPed specimens, displayed strain capability beyond matrix fracture and noncatastrophic failure behavior. However, the matrix fracture strain and ultimate tensile strength values of the HIPed SiC/RBSN were lower than those for the unHIPed SiC/RBSN composites. Improved first matrix cracking strength and lowered first matrix cracking strain for the HIPed SiC/RBSN composites can be explained by composite fracture theory (appendix). The loss in ultimate tensile strength of the HIPed composites can be attributed to fiber degradation during high temperature HIP consolidation.

## CONCLUSIONS

This study has shown that the density of the SiC/RBSN composites can be improved by increasing the preform density. However, this method is a negligibly effective method for improving mechanical strength of the SiC/RBSN composite. In contrast, HIPing with an additive can be used to fully densify SiC/RBSN and yield composites with measurably improved primary elastic modulus and first matrix cracking stress. However the ultimate tensile strength for the HIPed material can be lower than that for the unHIPed composite. This is related to the use of current SiC fibers which degrade at the HIP temperatures. When normalized by density, the primary elastic modulus and first matrix cracking stress values for the HIPed composites are lower than those for the unHIPed SiC/RBSN composites. This suggests that densified RBSN composite has no noticeable structural advantage over porous RBSN composite. However, one major advantage of the fully dense composite is expected to be improved oxidation resistance. It is possible though that long term oxidative stability of the porous RBSN composites can also be significantly improved by coating their external surfaces with a dense, impervious layer of SiC or $Si_3N_4$, or by using oxidation resistant SiC fibers as reinforcement.

## APPENDIX

The first matrix cracking stress in a unidirectionally reinforced ceramic matrix composite can be predicted from the Budiansky, Hutchinson and Evans theory (ref. 13). The relationship between the first matrix cracking stress, $\sigma_m^c$, and the constituent properties of the composite is,

$$\sigma_m^c = 2.98\left(K_c^m\right)^{2/3} \tau E_f V_f^2 (1 - V_f) \left\{ \frac{[1 - E_f V_f / E_m (1 - V_f)]^2}{E_m R} \right\}^{1/3}$$

where $\tau$ is the interfacial shear strength between the fiber and matrix, $K_c^m$ is the fracture toughness of matrix material, $V_f$ is the volume fraction of fibers, $E_f$ and $E_m$ are the elastic moduli of the fiber and matrix, respectively, and $R$ is the fiber radius. It is obvious from this equation that first matrix cracking stress varies directly with fracture toughness of the matrix and inversely with the modulus of the matrix. Both of these terms should increase with matrix density. In this study, although matrix density was increased from 1.67 to 3.05 gm/cc for the SiC/RBSN composites, first matrix cracking strength remained relatively the same. This strength behavior is possibly explained by the fact that the matrix toughness (unknown) and matrix modulus improvements have compensating effects in the above equation.

## REFERENCES


1. Heraud, L.; and Spriel, P.: High Toughness C-SiC and SiC-SiC Composites in Heat Engines. Whisker- and Fiber-Toughened Ceramics. R.A. Bradley, et al., eds., ASM International, 1988, pp. 217-224.

2. Andersson, C.A., et al.: Properties of Fiber-Reinforced Lanxide Alumina Matrix Composites. Whisker- and Fiber-Toughened Ceramics. R.A. Bradley, et al., eds., ASM International, 1988, pp. 209-216.

3. Bhatt, R.T.: The Properties of Silicon Carbide Fiber-Reinforced Silicon Nitride Composites. Whisker- and Fiber-Toughened Ceramics. R.A. Bradley, et al., ed., ASM International, 1988, pp. 199-208.

4. Bhatt, R.T.; and Phillips, R.E.: Laminate Behavior for SiC Fiber-Reinforced Reaction-Bonded Silicon Nitride Matrix Composites. NASA TM-101350, 1988.

5. Bhatt, R.T.: Method of Preparing Fiber-Reinforced Ceramic Materials. U.S. Patent No. 4689188, 1987.

6. Aveston, J.; Cooper, G.A.; and Kelly, A.: Single and Multiple Fracture. The Properties of Fiber Composites, Proceedings of the Conference. IPC Science and Technology Press Ltd., Surrey, England, 1971, pp. 15-26.

7. DiCarlo, J.A.; and Williams, W.: Dynamic Modulus and Damping of Boron, Silicon Carbide and Alumina Fibers. NASA TM-81422, 1980.

8. Richardson, D.W.: Modern Ceramic Engineering: Properties, Processing and Use in Design. Marcel Dekker, Inc., 1982.

9. Danforth, S.C.; Jennings, H.M.; and Richman, M.H.: The Influence of Microstructure on the Strength of Reaction-Bonded Silicon Nitride (RBSN). ACTA Metall., Vol. 27, Jan. 1979, pp. 123-130.

10. Moulson, A.J.: Review, Reaction-Bonded Silicon Nitride: Its Formation and Properties. J. Mater. Sci., Vol. 14, No. 5, 1979, pp. 1017-1051.

11. Jones, B.F.; and Lindley, M.W.: Strength, Density and Nitrogen Weight Gain Relationships for Reaction-Sintered Silicon Nitride. J. Mater. Sci., Vol. 10., No. 6, June 1975. pp. 967-972.

12. Jones, B.F.; Pittman, K.C.; and Lindley, M.W.: The Development of Strength in Reaction Sintered Silicon Nitride. J. Mater. Sci., Vol. 12, No. 3, Mar. 1977, pp. 563-576.

13. Budiansky, B.; Hutchison, J.W.; and Evans, A.G.: Matrix Fractured in Fiber-Reinforced Ceramics. J. Mech. Phys. Solids, Vol. 34, No. 2, 1986, pp. 167-189.

14. Deepley, C.G.; Hubert, J.M.; and Moore, N.C.: Dense Silicon Nitride. Powder Metall., Vol. 8, 1961, pp. 145-151.

15 Terwilliger, G.R.; and Lange, F.F.: Hot-Pressing Behavior of $Si_3N_4$. J. Am. Ceram. Soc., Vol. 57, No. 1, Jan. 1974, pp. 25-29.

16. Brennan, J.J.; and Prewo, K.M.: Silicon Carbide Fiber Reinforced Glass-Ceramic Matrix Composites Exhibiting High Strength and Toughness. J. Mater. Sci., Vol. 17, No. 8, Aug. 1982, pp. 2371-2375.

17. DiCarlo, J.A.: Creep of CVD SiC Fibers. J. Mater. Sci., Vol. 21, No. 1, Jan. 1986, pp. 217-224.

18. Foulds, W., et al.: Tough Silicon Nitride Matrix Composites Using Textron Silicon Carbide Monofilaments. Ceram. Eng. Sci. Proc., Vol. 10, No. 9-10, 1989. pp. 1083-1099.

TABLE 1. - ROOM TEMPERATURE PHYSICAL AND MECHANICAL PROPERTY DATA FOR AS-FABRICATED AND HIPed SiC/RBSN COMPOSITES

| Properties | As-fabricated SiC/RBSN | HIPed SiC/RBSN |
|---|---|---|
| Fiber fraction, vol % | 28±2 | 30±2 |
| Density, gm/cc | 2.3±0.1 | 3.05±0.05 |
| Porosity, vol % | 30±5 | 3±1 |
| Pore size, μm | 0.025 | --- |
| Primary elastic modulus, GPa | 193±7 | 293±3 |
| Tensile fracture strength, MPa | | |
| Matrix | 227±40 | 262±30 |
| Ultimate | 682±150 | 380±20 |
| Tensile fracture strain, percent | | |
| Matrix | ~0.11 | ~0.09 |
| Ultimate | ~0.45 | ~0.18 |
| Interfacial shear strength, MPa | 18±3 | 19±6 |

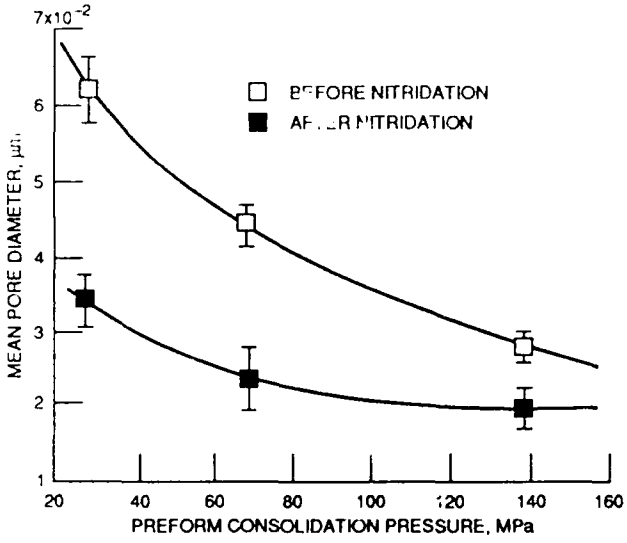


Figure 1. - Variation of matrix pore size with consolidation pressure for SiC/RBSN composites.

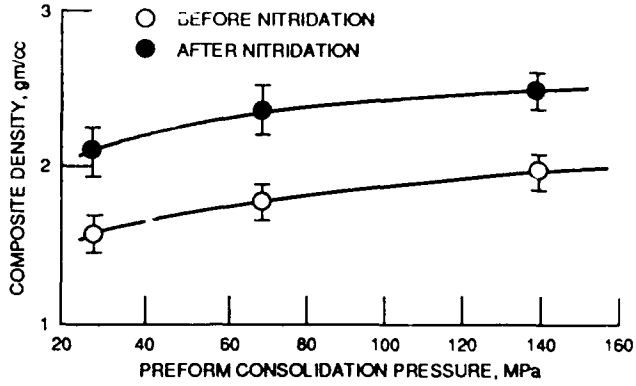


Figure 2. - Variation of composite density with consolidation pressure for SiC/RBSN composites.

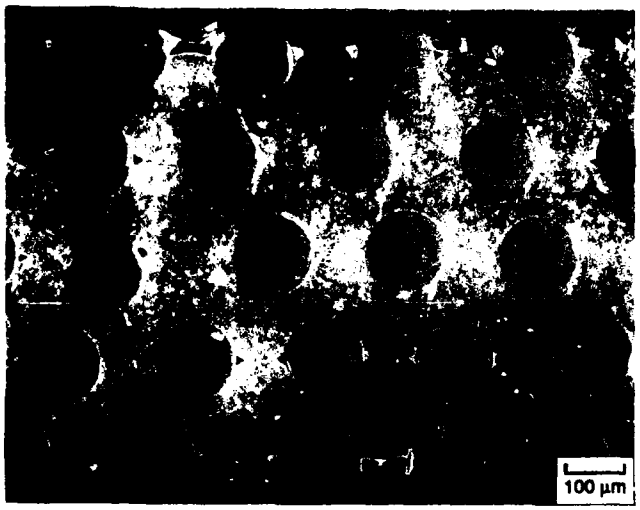


(a) 28 MPa.

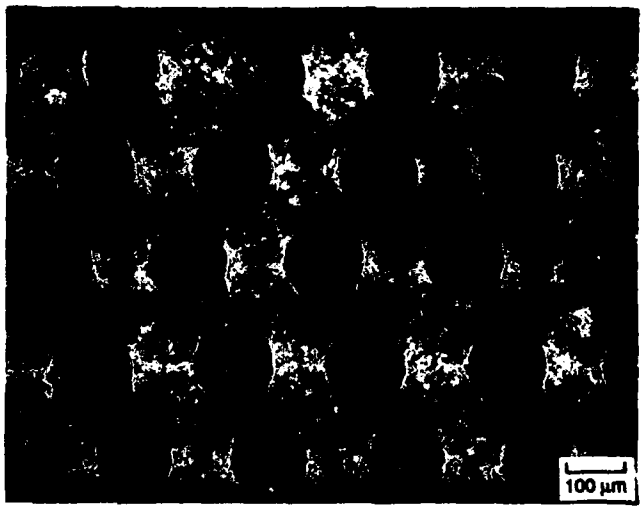


(b) 69 MPa.


(c) 138 MPa.

Figure 3. - SEM photographs of typical cross sections of 30 volume percent SiC/RBSN composites using preform consolidation pressures of (a) 28 MPa, (b) 69 MPa, and (c) 138 MPa.

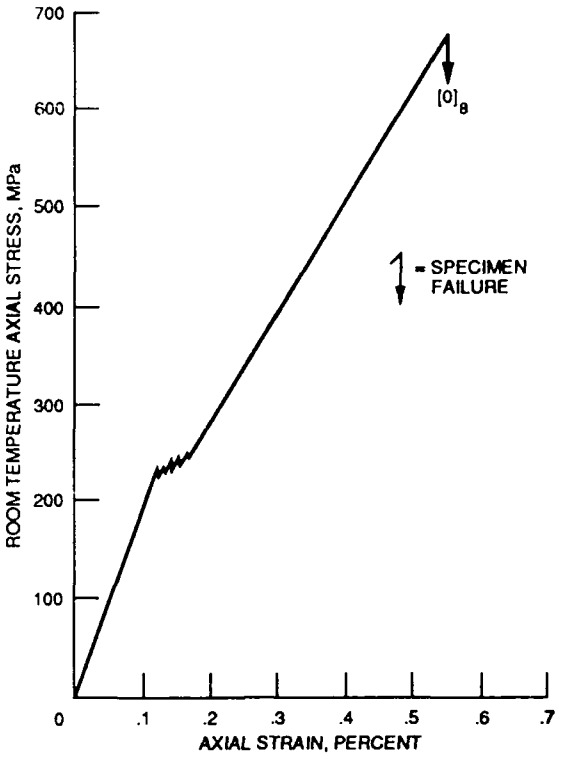


Figure 4. - Room temperature stress-strain curve for unidirectional SiC/RBSN composites.

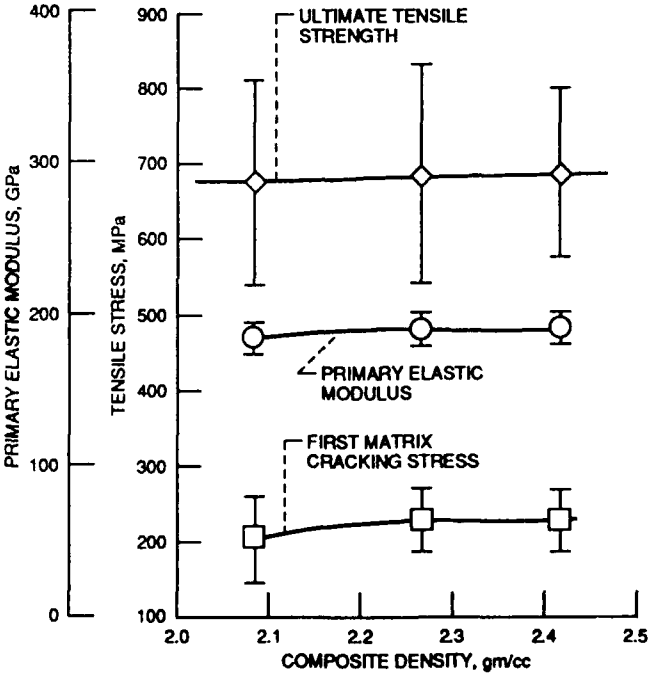


Figure 5. - Variation of primary elastic modulus, first matrix cracking stress, and ultimate tensile strength with composite density for SiC/RBSN composites.

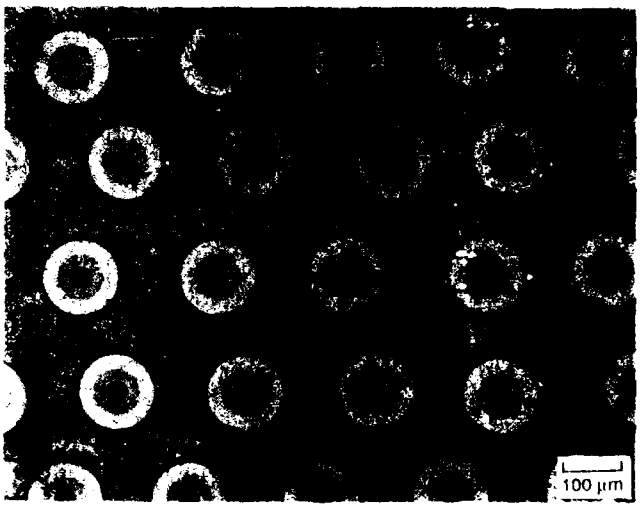


(a)


COATING

(b)

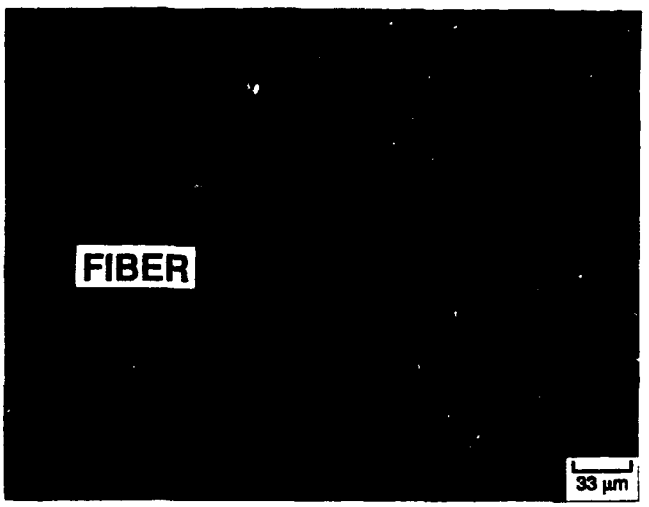


COATING

(c)

Figure 6. - (a) Typical cross-section of a HIPed SiC/RBSN composite showing the microstructure. Enlarged view of the fiber-matrix interface regions for (b) unHIPed and (c) HIPed composites

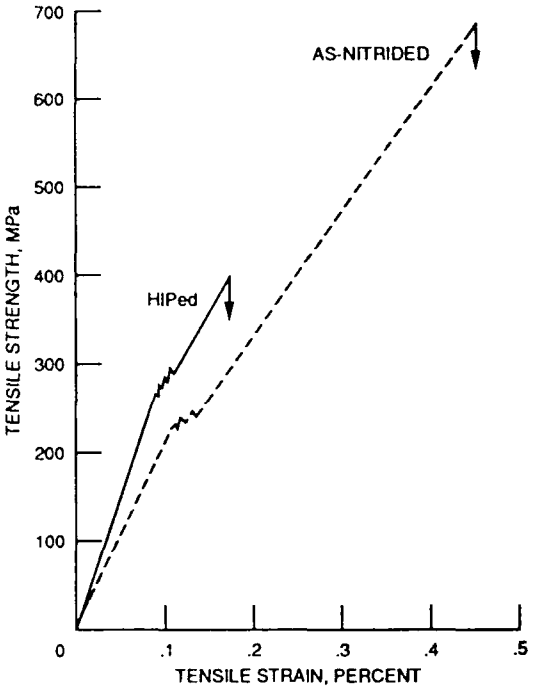


Figure 7. - Room temperature stress-strain curve for HIPed SiC/RBSN composites. Dashed line is the stress-strain curve for SiC/RBSN composites prior to HIPing.

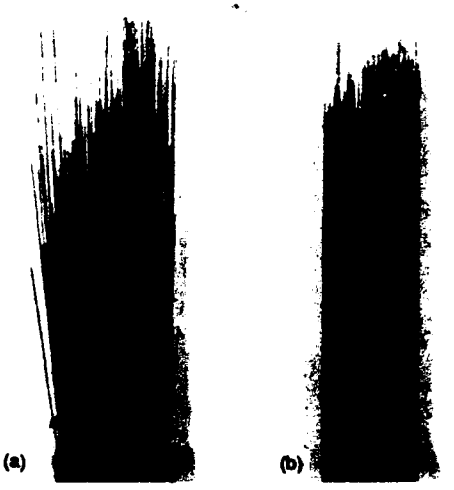


Figure 8. - Fractured tensile specimens of SiC/RBSN composites (a) unHIPed, (b) HIPed condition.

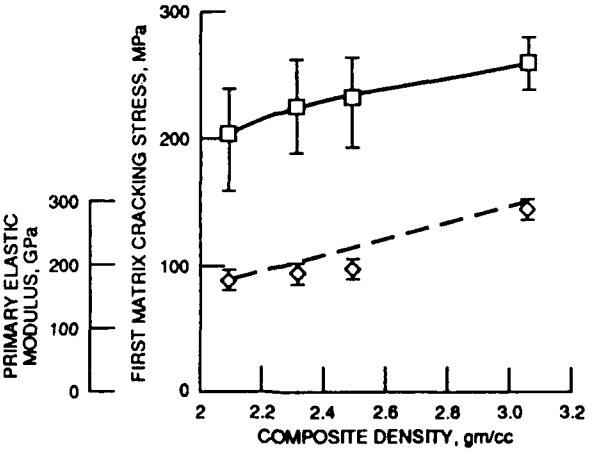


Figure 9. - Effect of composite density on the primary elastic modulus and first matrix cracking stress for SiC/RBSN composites. The dashed line indicates the effects of density on primary modulus as predicted by rule -of-mixtures.

NASA
National Aeronautics and Space Administration

# Report Documentation Page

| 1. Report No. | 2. Government Accession No. | 3. Recipient's Catalog No. |
|---|---|---|
| NASA TM-103098<br>AVSCOM TR-90-C-008 | | |

| 4. Title and Subtitle | 5. Report Date |
|---|---|
| Matrix Density Effects on the Mechanical Properties of SiC/RBSN Composites | 6. Performing Organization Code |

| 7. Author(s) | 8. Performing Organization Report No. |
|---|---|
| Ramakrishna T. Bhatt and James D. Kiser | E-5306 |

| 9. Performing Organization Name and Address | 10. Work Unit No. |
|---|---|
| NASA Lewis Research Center<br>Cleveland, Ohio 44135-3191<br>and<br>Propulsion Directorate<br>U.S. Army Aviation Research and Technology Activity—AVSCOM<br>Cleveland, Ohio 44135-3127 | 510-01-0A |
| | 11. Contract or Grant No. |
| | 13. Type of Report and Period Covered<br>Technical Memorandum |
| 12. Sponsoring Agency Name and Address<br>National Aeronautics and Space Administration<br>Washington, D.C. 20546-0001<br>and<br>U.S. Army Aviation Systems Command<br>St. Louis, Mo. 63120-1798 | 14. Sponsoring Agency Code |

15. Supplementary Notes

Prepared for the 14th Annual Conference on Composites and Advanced Ceramics sponsored by the American Ceramic Society, Cocoa Beach, Florida, January 14-17, 1990. Ramakrishna T. Bhatt, Propulsion Directorate, U.S. Army Aviation Research and Technology Activity—AVSCOM; James D. Kiser, NASA Lewis Research Center.

16. Abstract

The room temperature mechanical properties were measured for SiC fiber-reinforced reaction-bonded silicon nitride composites (SiC/RBSN) of different densities. The composites consisted of ~30 vol % uniaxially aligned 142 μm diameter SiC fibers (Textron SCS-6) in a reaction-bonded $Si_3N_4$ matrix. The composite density was varied by changing the consolidation pressure during RBSN processing and by hot isostatically pressing the SiC/RBSN composites. Results indicate that as the consolidation pressure was increased from 27 to 138 MPa, the average pore size of the nitrided composites decreased from 0.04 to 0.02 μm and the composite density increased from 2.07 to 2.45 gm/cc. Nonetheless, these improvements resulted in only small increases in the first matrix cracking stress, primary elastic modulus, and ultimate tensile strength values of the composites. In contrast, HIP consolidation of SiC/RBSN resulted in a fully dense material whose first matrix cracking stress and elastic modulus values were ~15 and ~50 percent higher, respectively, and ultimate tensile strength values were ~40 percent lower than those for unHIPed Sic/RBSN composites. The modulus behavior for all specimens can be explained by simple rule-of-mixture theory. Also, the loss in ultimate strength for the HIPed composites appears to be related to a degradation in fiber strength at the HIP temperature. However, the density effect on matrix fracture strength was much less than would be expected based on typical monolithic $Si_3N_4$ behavior, suggesting that composite theory is indeed operating. Possible practical implications of these observations are discussed.

| 17. Key Words (Suggested by Author(s)) | 18. Distribution Statement |
|---|---|
| Ceramic matrix composites; SiC fiber; $Si_3N_4$ matrix; HIPing; Mechanical properties | Unclassified – Unlimited<br>Subject Category 24 |

| 19. Security Classif. (of this report) | 20. Security Classif. (of this page) | 21. No. of pages | 22. Price* |
|---|---|---|---|
| Unclassified | Unclassified | 16 | A03 |

NASA FORM 1626 OCT 86

*For sale by the National Technical Information Service, Springfield, Virginia 22161